Applied Physics Letters

Incoherent phonon transport dominates heat conduction across van der Waals superlattices

Cite as: Appl. Phys. Lett. **121**, 022201 (2022); https://doi.org/10.1063/5.0096861
Submitted: 22 April 2022 • Accepted: 26 May 2022 • Published Online: 11 July 2022

Lu Zhao, Lijuan Zhang, Houfu Song, et al.

Applied Physics Letters ARTICLE scitation.org/journal/apl

Incoherent phonon transport dominates heat conduction across van der Waals superlattices

Cite as: Appl. Phys. Lett. **121**, 022201 (2022); doi: 10.1063/5.0096861
Submitted: 22 April 2022 · Accepted: 26 May 2022 ·
Published Online: 11 July 2022

View Online Export Citation CrossMark

Lu Zhao,[1] Lijuan Zhang,[1] Houfu Song,[1] Hongda Du,[2] Junqiao Wu,[3,4] Feiyu Kang,[1,2] and Bo Sun[1,2,a)]

AFFILIATIONS

[1]Tsinghua-Berkeley Shenzhen Institute, Tsinghua University, Shenzhen, Guangdong 518055, China
[2]Institute of Materials Research, Tsinghua Shenzhen International Graduate School, Guangdong Provincial Key Laboratory of Thermal Management Engineering and Materials, Shenzhen, Guangdong 518055, China
[3]Department of Materials Science and Engineering, University of California, Berkeley, Berkeley, California 94720, USA
[4]Materials Sciences, Lawrence Berkeley National Laboratory, Berkeley, California 94720, USA

[a)]Author to whom correspondence should be addressed: sun.bo@sz.tsinghua.edu.cn

ABSTRACT

Heat conduction mechanisms in superlattices could be different across different types of interfaces. Van der Waals superlattices are structures physically assembled through weak van der Waals interactions by design and may host properties beyond the traditional superlattices limited by lattice matching and processing compatibility, offering a different type of interface. In this work, natural van der Waals $(SnS)_{1.17}(NbS_2)_n$ superlattices are synthesized, and their thermal conductivities are measured by time-domain thermoreflectance as a function of interface density. Our results show that heat conduction of $(SnS)_{1.17}(NbS_2)_n$ superlattices is dominated by interface scattering when the coherent length of phonons is larger than the superlattice period, indicating that incoherent phonon transport dominates through-plane heat conduction in van der Waals superlattices even when the period is atomically thin and abrupt, in contrast to conventional superlattices. Our findings provide valuable insights into the understanding of the thermal behavior of van der Waals superlattices and devise approaches for effective thermal management of superlattices depending on the distinct types of interfaces.

Van der Waals (vdW) superlattices and heterostructures, vertically assembled using different monolayers or few-layer two-dimensional (2D) crystals, are emerging as a promising material system for electronic, photonic, and plasmonic studies.[1–6] Similar to conventional superlattices, interfaces play a key role in the behavior of vdW superlattices.[7,8] However, unlike conventional superlattices that are strongly covalently bonded across the interface, vdW superlattices are physically stacked together through weak van der Waals interactions, which allow rational design and flexible choices of combining highly distinct layers without consideration of lattice matching and processing compatibility and, thus, represent a distinctly different type of superlattice and interface.[9]

Thermal transport across interfaces is of vital importance in a diverse range of applications due to the increasing importance of thermal management, especially in devices based on superlattices and heterostructures where interface thermal transport typically dominates the heat conduction. In the past several decades, thermal transport in conventional superlattices has been extensively studied.[10–18] For example, Koh *et al.*[13] reported that interface thermal conductance increases with reduced superlattice period, suggesting that long-wavelength phonons are the dominant heat carriers in short-period AlN/GaN superlattices. In addition, Ravichandran *et al.*[16] observed that there is a crossover from incoherent to coherent phonon transport in oxide superlattices grown by molecular-beam epitaxy (MBE) when the coherent length of phonons is comparable to the period of the lattice. Despite these advances, it is unknown whether these heat conduction mechanisms are applicable to vdW superlattices and heterostructures because the interface in these structures is fundamentally different.

When studying thermal transport across the vdW superlattices, it is challenging to obtain the intrinsic phonon transport behavior across interfaces because the bottom-up assembled vdW superlattices normally suffer from interface contamination and turbostratic disorders.[19–23] Contamination-free and well-ordered vdW superlattices are required to study intrinsic phonon transport properties across these vdW interfaces. The family of misfit layered compounds are naturally occurring van der Waals superlattices that meet such requirements. They have a generic formula of $(MX)_{1+\delta}(TX_2)_n$, where M = Sn, Pb, Sb, Bi, or a rare earth element, T = group IV or V transition metals,

X = S or Se, and δ is the degree of structural mismatch between MX and TX_2.[24–26] In $(MX)_{1+\delta}(TX_2)_n$, each period is consisted of monolayer $(MX)_{1+\delta}$ and n layers of TX_2, where n can be tuned to adjust interface density. In addition, misfit layered compounds are a promising family of thermoelectric materials. It is, thus, worthwhile to study their thermal conduction properties.[27,28]

Here, we report that through-plane heat conduction in van der Waals superlattices is dominated by incoherent phonon transport. Using misfit layered compounds $(SnS)_{1.17}(NbS_2)_n$, we construct vdW superlattices with atomically sharp, contamination-free interfaces, which enable us to study the intrinsic phonon transport mechanism across the vdW interfaces. We show that incoherent phonons dominate heat transport in this system, despite that the phonon coherent length is larger than the superlattice period. This finding is in stark contrast to heat conduction in conventional AlAs/GaAs, $SrTiO_3/BaTiO_3$ (STO/BTO), and naturally occurred perovskite superlattices, where coherent phonon dominates when the period is short.[11,12,15,16] Our work provides valuable insights for the understanding of thermal behavior of vdW superlattices and heterostructures and devises approaches for effective thermal management across different types of interfaces.

We select $(SnS)_{1.17}(NbS_2)_n$ (n = 1, 2, 3) misfit layered compounds for this study, which were synthesized by chemical vapor transport.[24,29] The ratio of SnS and NbS_2 layers was tuned by controlling the temperature gradient in reaction quartz tubes. These three as-grown crystals are 1–5 mm-sized bulk samples. Further growth details can be found in the supplementary material. The structures of as-grown $(SnS)_{1.17}(NbS_2)_n$ (n = 1, 2, and 3) are shown in Figs. 1(a) and 1(b). All of the Bragg peaks are sharp and can be indexed to the (00l) family of planes, suggesting high crystallinity and preferred crystallographic alignment of the layers. As the number of inserted NbS_2 layer increases, the diffraction peaks present higher degree of consecutive structural orders [highlighted by the light-blue rectangle in Fig. 1(a)]. The existence of well-ordered, consecutively increased diffraction peaks indicates that superlattice structures of $(SnS)_{1.17}(NbS_2)_n$ were formed. Additional insertion of the NbS_2 layer results in a systematic increase in c-axis lattice parameter by 0.597 nm [Fig. 1(b)]. This result is consistent with the expected repeat unit thickness of monolayer of NbS_2 (0.598 nm).[30] In the inset of Fig. 1(b), we schematically illustrate the structure of $(SnS)_{1.17}(NbS2)_n$, which shows the incommensurate sublattices.

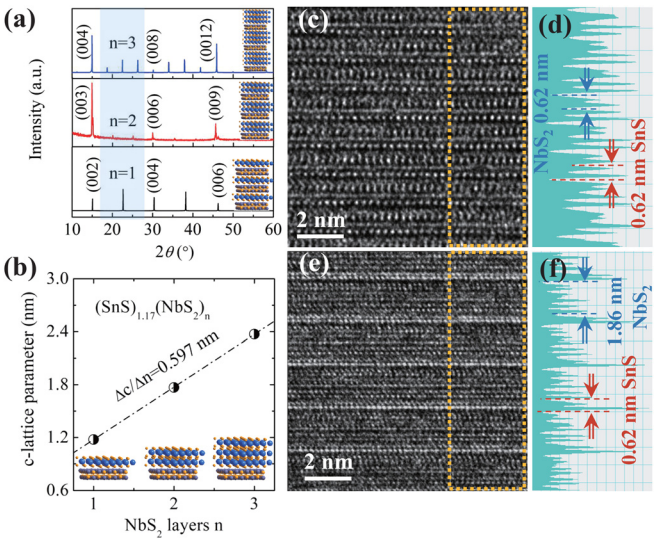

FIG. 1. (a) X-ray diffraction patterns for the $(SnS)_{1.17}(NbS_2)_n$ series. Selected (00l) reflections are labeled in the figure. The shaded region indicates that consecutive structural orders were obtained as the number of inserted NbS_2 layer increases. (b) c-Lattice parameter as a function of the number of NbS_2 layers. Representative HRTEM images for (c) and (d) $(SnS)_{1.17}NbS_2$ and (e) and (f) $(SnS)_{1.17}(NbS2)_3$ samples along the (010) direction. (d) and (f) Line profile images for $(SnS)_{1.17}NbS_2$ and $(SnS)_{1.17}(NbS_2)_3$ superlattices highlighted by white rectangle in (c) and (e), respectively.

High-resolution transmission electron microscopy confirms that $(SnS)_{1.17}NbS_2$ superlattice has the expected layering structure, which consists of vertically stacked SnS and NbS_2 sublayers, with atomically sharp and contamination-free interfaces [Figs. 1(c) and 1(d)]. The natural vdW superlattice feature and the spontaneous growth process lead to these high-quality interfaces.[31–34] Brighter regions correspond to greater scattering due to heavier atomic mass. The area of SnS, therefore, appears brighter than that of NbS_2. These two substructures display the same repeat thickness, 0.62 nm, according to the line profile [Fig. 1(d)]. The interfaces could provide considerable barriers to scatter heat-carrying phonons, despite that the coherent length of phonons is larger than the period of vdW superlattices, which will be discussed later. $(SnS)_{1.17}(NbS_2)_3$ superlattice consists of one-by-three vertically stacked SnS (0.62 nm) and NbS_2 (1.86 nm) sublayers, as shown in Figs. 1(e) and 1(f). The additional increase in repeat unit thickness (0.62 nm) is slightly larger than the result (0.597 nm) obtained from x-ray diffraction [Fig. 1(b)]. No obvious turbostratic disorder was observed in the $(SnS)_{1.17}(NbS_2)_n$ series.[20]

We measured the through-plane thermal conductivity, Λ, of the $(SnS)_{1.17}(NbS_2)_n$ series and SnS and NbS_2 single crystals as a function of temperature using time-domain thermoreflectance (TDTR),[35,36] which has been widely used in measuring thermal conductivity of superlattices, 2D materials, etc.[37–40] In the typical TDTR measurement, pump laser periodically heats the sample, probe laser tracks the reflectance of surface as the temperature changes, and an analytical solution of multilayer heat diffusion equation is used to fit the derived signal to extract the sample's unknown thermal conductivity [Fig. 2(a)]. To ensure the accuracy and consistency of our measurement, we systematically performed sensitivity calculations for each parameter [Figs. 2(b) and 2(c)]. We employed a large $1/e^2$ radii w_0 (10.3 μm) of the laser beam to ensure 1D heat diffusion along the through-plane direction. The predicted thermal penetration depth is a few hundred nanometers for all samples even at the lowest modulation frequency, which is much smaller than the thickness of these samples (20–120 μm). The samples were placed in the sample chamber full with argon before the deposition of 80-nm-thick Al transducer and measurement in the high vacuum cryostat to prevent from oxidation and contamination.

The through-plane thermal conductivity of bulk SnS, NbS_2, and superlattices is measured from 80 to 500 K and summarized in Fig. 3(a). Λ of single crystalline SnS is inversely proportional to temperature, which agrees well with the predictions from Boltzmann transport equation (BTE) and temperature dependent effective potential (TDEP) calculations (Fig. S2 in supplementary material).[41] This T^{-1} dependence suggests that the heat conduction is dominated by

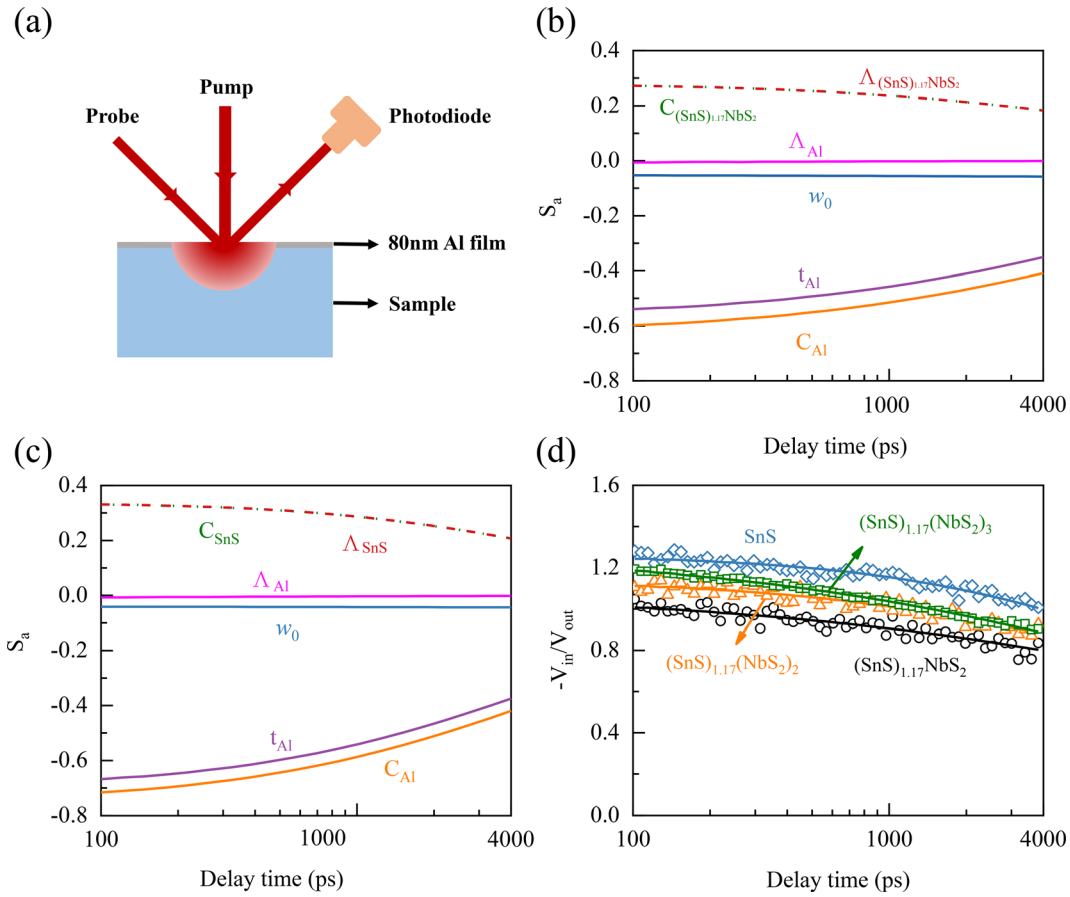

FIG. 2. (a) Schematic figure of the principles of TDTR measurement. Sensitivity of TDTR measurement of $(SnS)_{1.17}NbS_2$ (b) and SnS (c) to volumetric heat capacity (green dashed line), thermal conductivity (red dashed line), thermal conductivity of Al (magenta line), spot size of laser beam (blue line), thickness of the Al film (purple line), and volumetric heat capacity of Al (orange line) with the $1/e^2$ radii w_0 of the laser beams of 10.3 μm and the modulation frequency of 10.1 MHz. (d) Best fit for measured signal of SnS (blue), $(SnS)_{1.17}NbS_2$ (dark), $(SnS)_{1.17}(NbS_2)_2$ (orange), and $(SnS)_{1.17}(NbS_2)_3$ (green) at 300 K.

phonon–phonon scattering. On the contrary, Λ of NbS_2 monotonically increases with temperature, suggesting that the electron–phonon coupling plays an important role in the through-plane thermal transport.[42] The measured thermal conductivity of bulk SnS and NbS_2 might provide one of the earliest reference for further research on the mechanism of heat conduction of phonons, electrons, and their coupling in through-plane of vdW materials. Λ reduces with decreasing temperature for all $(SnS)_{1.17}(NbS_2)_n$ samples, which is typical for long-period superlattices, indicating that the dominate phonon scattering mechanism is interface scattering.[13,16] We ignored the contribution of electron–phonon coupling in NbS_2 to interface thermal conductance, as we postulate that electrical thermal conductivity of NbS_2 is small comparing with its lattice thermal conductivity, suggested by a similar material TaS_2.[42] Moreover, we find that Λ reduces monotonically as the interface density increases. At room temperature, Λ for bulk single crystalline SnS and NbS_2 is 1.37 and 1.64 W m^{-1} K^{-1} and decreases to 0.82, 0.62, and 0.44 W m^{-1} K^{-1} for $(SnS)_{1.17}(NbS_2)_3$, $(SnS)_{1.17}(NbS_2)_2$, and $(SnS)_{1.17}NbS_2$ as the interface density increases to 0.81 (n = 3), 1.08 (n = 2), and 1.61 nm^{-1} (n = 1), respectively, indicating no appearance of increase in lattice thermal conductivity in the high interface density regime where phonons transport in wave-like coherent scattering.

Phonon coherent length serves as an important parameter to determine the dividing line of incoherent and coherent transport. The wave nature of phonons should be considered at the high interface density regime, where the supperlattice period is comparable to the coherent length, and the phonon waves transport across the atomically abrupt interface without external scatterings.[17,43] To compare with the conventional covalent superlattices where coherent phonon dominates when the period is short,[44] we calculated the phonon coherent length of $(SnS)_{1.17}(NbS_2)_n$ superlattice to predict whether the coherent heat transport occurs at or beyond their phonon coherent length. The phonon coherent length was calculated using a method reported previsouly.[45] An averaged Debye-like dispersion was assumed for all the acoustic branches; the contributions of the optical branches were ignored.[16] Here, we use the coherence length of SnS as a qualitative estimate, and it is important to realize that one must consider the full dispersion for fully accurate coherence-length calculations. The zone edge cutoff frequencies and group velocities for SnS were obtained from references.[46] The calculated coherence length of SnS for

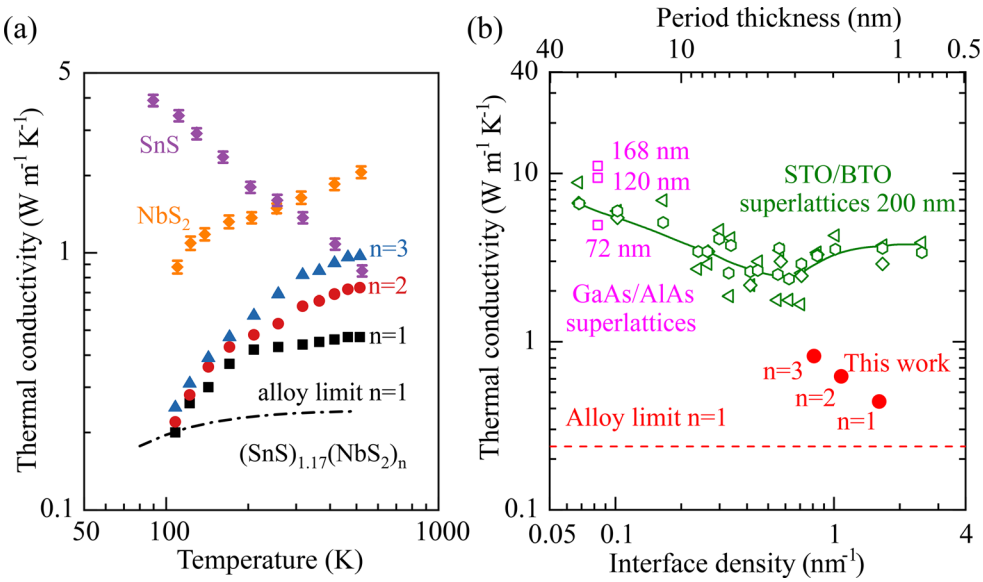

FIG. 3. (a) Through-plane thermal conductivity as a function of temperature for the $(SnS)_{1.17}(NbS_2)_n$ series. The black dashed line refers to the alloy limit of $(SnS)_{1.17}NbS_2$ calculated using the Cahill–Pohl model.[47] The purple and orange diamonds refer to the bulk SnS and NbS_2. (The uncertainty of TDTR measurement is lower than 7%.) (b) Measured room-temperature thermal conductivity values for various superlattices as a function of interface density. The room-temperature thermal conductivity of GaAs/AlAs superlattice[15] and $(SrTiO_3)_m/(BaTiO_3)_n$ superlattice[16] is included for comparison.

longitudinal and transverse modes is 6.2 and 5 nm, respectively. As the interface density increases, the through-plane thermal conductivity at room temperature continuously reduces, indicating that the heat conduction is dominantly limited by interface scattering, even when the superlattice period is atomically thin and shorter than the coherent length of phonons [Fig. 3(b)]. This result is in contrast to the mechanism of heat conduction observed in AlAs/GaAs and BTO/STO superlattices, where coherent phonons dominate the heat conduction when the superlattice period is short.[15,16]

Since phonons are not coherently correlated in different layers of the $(SnS)_{1.17}(NbS_2)_n$ superlattice, interface scattering plays an important role in heat conduction due to the particle-like behavior of phonons; thereby, the whole superlattice can be modeled as series of interface resistance with bulk SnS and NbS_2 thermal resistance added in series. In order to obtain more insights about the heat conduction mechanism in the vdW superlattices, the thermal conductance G across the SnS/NbS_2 interface is estimated using the following formula:[13]

$$\frac{2}{G} = \frac{h_{SnS} + h_{NbS_2}}{\Lambda_{superlattice}} - \frac{h_{SnS}}{\Lambda_{SnS}} - \frac{h_{NbS_2}}{\Lambda_{NbS_2}}, \quad (1)$$

where h_{SnS}, h_{NbS_2}, $\Lambda_{superlattice}$, Λ_{SnS}, and Λ_{NbS_2} are the thickness of the SnS sublayer, thickness of the NbS_2 sublayer, and the thermal conductivity of the entire superlattice of SnS[46] and of NbS_2, respectively. The derived room-temperature G is plotted in Fig. 4. As the interface density increases, the thermal conductance G shows a monotonous reduction. At room temperature, the thermal conductance G for the sample with the interface density of $0.81\,nm^{-1}$ $(n = 3)$ is $4.21\,GW\,m^{-2}\,K^{-1}$, and it decreases to $1.33\,GW\,m^{-2}\,K^{-1}$ as the interface density increases to $1.61\,nm^{-1}$ $(n = 1)$. This could be explained as long-wavelength phonons being scattered more strongly when the interface density is large, which is in opposite to the coherent phonon scattering behavior in conventional superlattices.[13,48–50] The considerable decrease in interface thermal conductance indicates that the major scattering mechanism is interface scattering in $(SnS)_{1.17}(NbS_2)_n$ superlattices (Fig. 4).

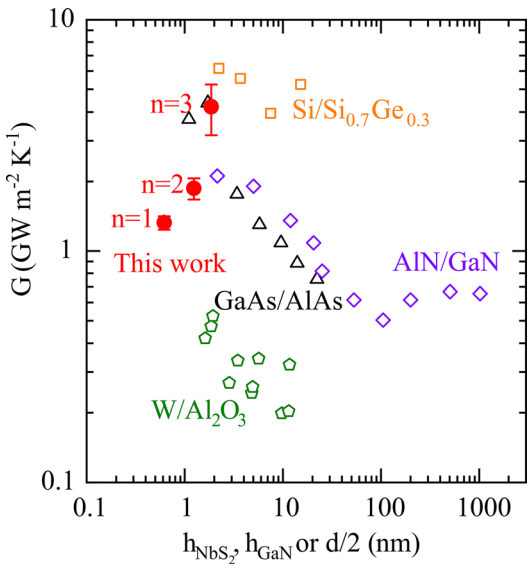

FIG. 4. Room-temperature interface thermal conductance of $(SnS)_{1.17}(NbS_2)_n$ series (solid circles). The interface thermal conductance of AlN/GaN superlattices (open diamonds),[13] $Si/Si_{0.7}Ge_{0.3}$ superlattices (open squares),[50] GaAs/AlAs superlattices (open triangles),[48] and W/Al_2O_3 multilayers (open pentagons)[49] is included for comparison and is plotted as a function of h_{GaN} or half of the period, d/2.

One of the important predictions regarding interface thermal conductance G in short-period superlattices is that G increases with the reduction in superlattice period due to the coherent transport of long-wavelength phonons.[13] Such behavior has been observed in short-period $Si/Si_{0.7}Ge_{0.3}$ superlattices,[50] GaAs/AlAs superlattices,[48] W/Al_2O_3 multilayers,[49] and perovskite superlattices.[11] However, in our misfit vdW superlattices, we see the opposite trend that G reduces following the reduction of superlattice period, even though the interface is atomically thin and smaller than the coherent length of phonons. We postulate that this obvious contrast stems from the difference in bonding types at the interfaces. Conventional fabrication for superlattices and heterostructures by epitaxial growth relies on strong covalent bonding across the interface. Symmetry, lattice mismatching and deposition induced strain/defects at and beyond the interfaces result in a strong scattering of phonons in the propagation of phonons across epitaxy superlattices.[51,52] As the coherent length of phonons is comparable or larger than the superlattice period, long wavelength phonons will transport coherently across the interface in conventional superlattices, resulting in enhancement of thermal transport.[13,48–50] However, in our vdW superlattices, the interface is weakly bonded by the van der Waals interactions, and the lattice symmetry is broken across the incommensurate sublayers, although the superlattice period is atomically thin. Thus, phonons will lose their coherence when propagating through such interfaces, leading to the reduction of thermal conductance and an incoherent phonon transport.

Our result is fundamentally different from the artificial MoS_2/WS_2 vdW superlattices calculated by Guo *et al.*,[44] where they computed that phonon can transport coherently across interfaces. In the case of MoS_2/WS_2, the lattice constant of MoS_2 (one layer: a = 0.3125 nm; two layers: a = 0.3126 nm) and WS_2 (one layer: a = 0.3125 nm; two layers: a = 0.3125 nm) is nearly the same, so they can form superlattices with minimum lattice mismatch.[53] Thus, the interfaces in MoS_2/WS_2 superlattice maintain lattice symmetry that could host coherent phonon transport. In our case, the lattice mismatch between SnS (a = 0.5673 nm) and NbS_2 (a = 0.3321 nm)[26] is large, and hence, phonon transport in $(SnS)_{1.17}(NbS_2)_n$ superlattices is governed by the discontinuity in symmetry, which destroys the wave interference and changes the nature of phonon transport from coherent to diffusive when the phonons propagate across the interfaces.[54] Our results indicate that incoherent phonons dominate through-plane heat conduction, even when the period is atomically thin, clean, and abrupt, for lattice mismatched vdW superlattices. In real-world applications, vdW superlattices and heterostructures are predominately lattice mismatched,[55] and thus, our results and conclusion could be applied to the broad family of vdW superlattices and heterostructures.

In summary, natural van der Waals $(SnS)_{1.17}(NbS_2)_n$ superlattices are synthesized by chemical vapor transport. The through-plane thermal conductivity, Λ, of the $(SnS)_{1.17}(NbS_2)_n$ series is measured by time-domain thermoreflectance, showing a continuous reduction as the interface density increases. The continuous reduction of thermal conductivity is related to additional interfacial thermal resistance induced by the insertion of more NbS_2 layers, which reveals that coherent phonon transport is not important in heat conduction in vdW superlattices. In contrast to conventional covalent superlattices where coherent phonon dominates when the period is short, our result of incoherent phonon transport dominating heat conduction in vdW superlattices provides an attractive and broadly applicable insight that heat transport mechanisms in superlattices and heterostructures are different depending on the specific physical property of interfaces.

See the supplementary material for the sample preparation, TDTR measurement, and calculations for alloy limit and coherence length.

B.S., L. Zhang, L. Zhao, and H.S. acknowledge the support of Guangdong Natural Science Foundation (No. 2019A1515010868), the National Natural Science Foundation of China (No. 12004211), the Shenzhen Science and Technology Program (No. RCYX20200714114643187), and Tsinghua Shenzhen International Graduate School (No. QD2021008N). L. Zhang acknowledges the support from the National Natural Science Foundation of China (No. 52002206), the Postdoctoral Science Foundation (No. 2019M650669), and the Shenzhen Science and Technology Program (No. RCBS20200714114857131). The authors thank the support from the Testing Technology Center of Materials and Devices in Tsinghua Shenzhen International Graduate School and Analytical Instrumentation Center in Peking University Shenzhen Graduate School.

AUTHOR DECLARATIONS

Conflict of Interest

The authors have no conflicts to disclose.

Author Contributions

Lu Zhao: Data curation (equal); Formal analysis (equal). **Lijuan Zhang:** Investigation (equal); Methodology (equal); Writing – original draft (equal). **Houfu Song:** Validation (equal). **Hongda Du:** Resources (equal). **Junqiao Wu:** Supervision (equal); Writing – review and editing (equal). **Feiyu Kang:** Supervision (equal). **Bo Sun:** Formal analysis (lead); Funding acquisition (lead); Supervision (lead); Writing – review and editing (lead).

DATA AVAILABILITY

The data that support the findings of this study are available from the corresponding author upon reasonable request.

REFERENCES

[1] T. J. Echtermeyer, L. Britnell, P. K. Jasnos, A. Lombardo, R. V. Gorbachev, A. N. Grigorenko, A. K. Geim, A. C. Ferrari, and K. S. Novoselov, "Strong plasmonic enhancement of photovoltage in graphene," Nat. Commun. **2**, 458 (2011).

[2] Y. Liu, H. Zhou, R. Cheng, W. Yu, Y. Huang, and X. Duan, "Highly flexible electronics from scalable vertical thin film transistors," Nano Lett. **14**(3), 1413–1418 (2014).

[3] F. Withers, O. Del Pozo-Zamudio, A. Mishchenko, A. P. Rooney, A. Gholinia, K. Watanabe, T. Taniguchi, S. J. Haigh, A. K. Geim, A. I. Tartakovskii, and K. S. Novoselov, "Light-emitting diodes by band-structure engineering in van der Waals heterostructures," Nat. Mater. **14**(3), 301–306 (2015).

[4] T. Yang, B. Zheng, Z. Wang, T. Xu, C. Pan, J. Zou, X. Zhang, Z. Qi, H. Liu, Y. Feng, W. Hu, F. Miao, L. Sun, X. Duan, and A. Pan, "Van der Waals epitaxial growth and optoelectronics of large-scale WSe_2/SnS_2 vertical bilayer p–n junctions," Nat. Commun. **8**, 1906 (2017).

[5] W. J. Yu, Z. Li, H. Zhou, Y. Chen, Y. Wang, Y. Huang, and X. Duan, "Vertically stacked multi-heterostructures of layered materials for logic transistors and complementary inverters," Nat. Mater. **12**(3), 246–252 (2013).

[6]W. J. Yu, Y. Liu, H. Zhou, A. Yin, Z. Li, Y. Huang, and X. Duan, "Highly efficient gate-tunable photocurrent generation in vertical heterostructures of layered materials," Nat. Nanotechnol. **8**(12), 952–958 (2013).
[7]M. C. Asensio and M. Batzill, "Interfaces and heterostructures of van der Waals materials," J. Phys. **28**(49), 490301 (2016).
[8]E. T. Swartz and R. O. Pohl, "Thermal resistance at interfaces," Appl. Phys. Lett. **51**(26), 2200–2202 (1987).
[9]Y. Liu, N. O. Weiss, X. Duan, H.-C. Cheng, Y. Huang, and X. Duan, "Van der Waals heterostructures and devices," Nat. Rev. Mater. **1**, 16042 (2016).
[10]R. Cheaito, C. A. Polanco, S. Addamane, J. Zhang, A. W. Ghosh, G. Balakrishnan, and P. E. Hopkins, "Interplay between total thickness and period thickness in the phonon thermal conductivity of superlattices from the nanoscale to the microscale: Coherent versus incoherent phonon transport," Phys. Rev. B **97**(8), 085306 (2018).
[11]A. D. Christodoulides, P. Guo, L. Dai, J. M. Hoffman, X. Li, X. Zuo, D. Rosenmann, A. Brumberg, M. G. Kanatzidis, R. D. Schaller, and J. A. Malen, "Signatures of coherent phonon transport in ultralow thermal conductivity two-dimensional Ruddlesden–Popper phase perovskites," ACS Nano **15**(3), 4165–4172 (2021).
[12]N. M. Dawley, E. K. Pek, C.-H. Lee, E. J. Ragasa, X. Xiong, K. Lee, S. R. Phillpot, A. V. Chernatynskiy, D. G. Cahill, and D. G. Schlom, "Thermal conductivity of the $n = 1$–5 and 10 members of the $(SrTiO_3)_nSrO$ Ruddlesden–Popper superlattices," Appl. Phys. Lett. **118**(9), 091904 (2021).
[13]Y. K. Koh, Y. Cao, D. G. Cahill, and D. Jena, "Heat-transport mechanisms in superlattices," Adv. Funct. Mater. **19**(4), 610–615 (2009).
[14]B. Latour, S. Volz, and Y. Chalopin, "Microscopic description of thermal-phonon coherence: From coherent transport to diffuse interface scattering in superlattices," Phys. Rev. B **90**(1), 014307 (2014).
[15]M. N. Luckyanova, J. Garg, K. Esfarjani, A. Jandl, M. T. Bulsara, A. J. Schmidt, A. J. Minnich, S. Chen, M. S. Dresselhaus, Z. Ren, E. A. Fitzgerald, and G. Chen, "Coherent phonon heat conduction in superlattices," Science **338**(6109), 936–939 (2012).
[16]J. Ravichandran, A. K. Yadav, R. Cheaito, P. B. Rossen, A. Soukiassian, S. J. Suresha, J. C. Duda, B. M. Foley, C.-H. Lee, Y. Zhu, A. W. Lichtenberger, J. E. Moore, D. A. Muller, D. G. Schlom, P. E. Hopkins, A. Majumdar, R. Ramesh, and M. A. Zurbuchen, "Crossover from incoherent to coherent phonon scattering in epitaxial oxide superlattices," Nat. Mater. **13**(2), 168–172 (2014).
[17]M. V. Simkin and G. D. Mahan, "Minimum thermal conductivity of superlattices," Phys. Rev. Lett. **84**(5), 927 (2000).
[18]Y. Wang, H. Huang, and X. Ruan, "Decomposition of coherent and incoherent phonon conduction in superlattices and random multilayers," Phys. Rev. B **90**(16), 165406 (2014).
[19]C. Chiritescu, D. G. Cahill, C. Heideman, Q. Lin, C. Mortensen, N. T. Nguyen, D. Johnson, R. Rostek, and H. Böttner, "Low thermal conductivity in nanoscale layered materials synthesized by the method of modulated elemental reactants," J. Appl. Phys. **104**(3), 033533 (2008).
[20]C. Chiritescu, D. G. Cahill, N. Nguyen, D. Johnson, A. Bodapati, P. Keblinski, and P. Zschack, "Ultralow thermal conductivity in disordered, layered WSe_2 crystals," Science **315**(5810), 351–353 (2007).
[21]N. S. Gunning, J. Feser, M. Beekman, D. G. Cahill, and D. C. Johnson, "Synthesis and thermal properties of solid-state structural isomers: Ordered intergrowths of SnSe and $MoSe_2$," J. Am. Chem. Soc. **137**(27), 8803–8809 (2015).
[22]S. J. Haigh, A. Gholinia, R. Jalil, S. Romani, L. Britnell, D. C. Elias, K. S. Novoselov, L. A. Ponomarenko, A. K. Geim, and R. Gorbachev, "Cross-sectional imaging of individual layers and buried interfaces of graphene-based heterostructures and superlattices," Nat. Mater. **11**(9), 764–767 (2012).
[23]J. J. Schwartz, H.-J. Chuang, M. R. Rosenberger, S. V. Sivaram, K. M. McCreary, B. T. Jonker, and A. Centrone, "Chemical identification of interlayer contaminants within van der Waals heterostructures," ACS Appl. Mater. Interfaces **11**(28), 25578–25585 (2019).
[24]W. Bai, P. Li, S. Ju, C. Xiao, H. Shi, S. Wang, S. Qin, Z. Sun, and Y. Xie, "Monolayer behavior of NbS_2 in natural van der Waals heterostructures," J. Phys. Chem. Lett. **9**(22), 6421–6425 (2018).
[25]A. R. H. F. Ettema, C. Haas, and T. S. Turner, "Strong multiple resonances in the photoemission spectra of transition-metal-layer and misfit-layer compounds," Phys. Rev. B **47**(19), 12794 (1993).
[26]C. M. Fang, A. R. H. F. Ettema, C. Haas, G. A. Wiegers, H. van Leuken, and R. A. de Groot, "Electronic structure of the misfit-layer compound $(SnS)_{1.17}NbS_2$ deduced from band-structure calculations and photoelectron spectra," Phys. Rev. B **52**(4), 2336 (1995).
[27]C. Wan, Y. Wang, N. Wang, W. Norimatsu, M. Kusunoki, and K. Koumoto, "Development of novel thermoelectric materials by reduction of lattice thermal conductivity," Sci. Technol. Adv. Mater. **11**, 044306 (2010).
[28]H. Zhu, C. Zhao, P. Nan, X-m. Jiang, J. Zhao, B. Ge, C. Xiao, and Y. Xie, "Intrinsically low lattice thermal conductivity in natural superlattice $(Bi_2)_m(Bi_2Te_3)_n$ thermoelectric materials," Chem. Mater. **33**(4), 1140–1148 (2021).
[29]T. Terashima and N. Kojima, "Magnetic properties of incommensurate layer compounds $(CeS)_{1.2}NbS_2$ and $(CeS)_{0.6}NbS_2$," J. Phys. Soc. Jpn. **61**(9), 3303–3312 (1992).
[30]C. J. Carmalt, T. D. Manning, I. P. Parkin, E. S. Peters, and A. L. Hector, "Formation of a new (1T) trigonal NbS_2 polytype via atmospheric pressure chemical vapour deposition," J. Mater. Chem. **14**(3), 290–291 (2004).
[31]D. Hu, G. Xu, L. Xing, X. Yan, J. Wang, J. Zheng, Z. Lu, P. Wang, X. Pan, and L. Jiao, "Two-dimensional semiconductors grown by chemical vapor transport," Angew. Chem., Int. Ed. **56**(13), 3611–3615 (2017).
[32]H. Li, J. Liu, N. Guo, L. Xiao, H. Zhang, S. Zhou, Y. Wu, and S. Fan, "Seeded growth of high-quality transition metal dichalcogenide single crystals via chemical vapor transport," CrystEngComm **22**(46), 8017–8022 (2020).
[33]L. Xing, X. Yan, J. Zheng, G. Xu, Z. Lu, L. Liu, J. Wang, P. Wang, X. Pan, and L. Jiao, "Highly crystalline $ReSe_2$ atomic layers synthesized by chemical vapor transport," InfoMat **1**(4), 552–558 (2019).
[34]Y. Zhao and S. Jin, "Controllable water vapor assisted chemical vapor transport synthesis of WS_2–MoS_2 heterostructure," ACS Mater. Lett. **2**(1), 42–48 (2020).
[35]D. G. Cahill, "Analysis of heat flow in layered structures for time-domain thermoreflectance," Rev. Sci. Instrum. **75**(12), 5119–5122 (2004).
[36]B. Sun and Y. Kan Koh, "Understanding and eliminating artifact signals from diffusely scattered pump beam in measurements of rough samples by time-domain thermoreflectance (TDTR)," Rev. Sci. Instrum. **87**(6), 064901 (2016).
[37]J. Ju, B. Sun, G. Haunschild, B. Loitsch, B. Stoib, M. S. Brandt, M. Stutzmann, Y. K. Koh, and G. Koblmüller, "Thermoelectric properties of In-rich InGaN and InN/InGaN superlattices," AIP Adv. **6**(4), 045216 (2016).
[38]B. Sun, X. Gu, Q. Zeng, X. Huang, Y. Yan, Z. Liu, R. Yang, and Y. K. Koh, "Temperature dependence of anisotropic thermal-conductivity tensor of bulk black phosphorus," Adv. Mater. **29**(3), 1603297 (2017).
[39]B. Sun, G. Haunschild, C. Polanco, J. Ju, L. Lindsay, G. Koblmüller, and Y. K. Koh, "Dislocation-induced thermal transport anisotropy in single-crystal group-III nitride films," Nat. Mater. **18**(2), 136–140 (2019).
[40]B. Sun, S. Niu, R. P. Hermann, J. Moon, N. Shulumba, K. Page, B. Zhao, A. S. Thind, K. Mahalingam, and J. Milam-Guerrero, "High frequency atomic tunneling yields ultralow and glass-like thermal conductivity in chalcogenide single crystals," Nat. Commun. **11**, 6039 (2020).
[41]T. Lanigan-Atkins, S. Yang, J. L. Niedziela, D. Bansal, A. F. May, A. A. Puretzky, J. Y. Y. Lin, D. M. Pajerowski, T. Hong, S. Chi, G. Ehlers, and O. Delaire, "Extended anharmonic collapse of phonon dispersions in SnS and SnSe," Nat. Commun. **11**, 4430 (2020).
[42]H. Liu, C. Yang, B. Wei, L. Jin, A. Alatas, A. Said, S. Tongay, F. Yang, A. Javey, and J. Hong, "Anomalously suppressed thermal conduction by electron-phonon coupling in charge-density-wave tantalum disulfide," Adv. Sci. **7**(11), 1902071 (2020).
[43]Z. Zhang, Y. Guo, M. Bescond, J. Chen, M. Nomura, and S. Volz, "Coherent thermal transport in nano-phononic crystals: An overview," APL Mater. **9**(8), 081102 (2021).
[44]R. Guo, Y.-D. Jho, and A. J. Minnich, "Coherent control of thermal phonon transport in van der Waals superlattices," Nanoscale **10**(30), 14432–14440 (2018).
[45]G. Chen, "Size and interface effects on thermal conductivity of superlattices and periodic thin-film structures," J. Heat Transfer **119**(2), 220–229 (1997).
[46]R. Guo, X. Wang, Y. Kuang, and B. Huang, "First-principles study of anisotropic thermoelectric transport properties of IV-VI semiconductor compounds SnSe and SnS," Phys. Rev. B **92**(11), 115202 (2015).
[47]D. G. Cahill, S. K. Watson, and R. O. Pohl, "Lower limit to the thermal conductivity of disordered crystals," Phys. Rev. B **46**(10), 6131 (1992).

[48]W. S. Capinski, H. J. Maris, T. Ruf, M. Cardona, K. Ploog, and D. S. Katzer, "Thermal-conductivity measurements of GaAs/AlAs superlattices using a picosecond optical pump-and-probe technique," Phys. Rev. B **59**(12), 8105 (1999).
[49]R. M. Costescu, D. G. Cahill, F. H. Fabreguette, Z. A. Sechrist, and S. M. George, "Ultra-low thermal conductivity in W/Al_2O_3 nanolaminates," Science **303**(5660), 989–990 (2004).
[50]S. T. Huxtable, A. R. Abramson, C.-L. Tien, A. Majumdar, C. LaBounty, X. Fan, G. Zeng, J. E. Bowers, A. Shakouri, and E. T. Croke, "Thermal conductivity of Si/SiGe and SiGe/SiGe superlattices," Appl. Phys. Lett. **80**(10), 1737–1739 (2002).
[51]Y. Chen, D. Li, J. R. Lukes, Z. Ni, and M. Chen, "Minimum superlattice thermal conductivity from molecular dynamics," Phys. Rev. B **72**(17), 174302 (2005).
[52]B. Yang and G. Chen, "Partially coherent phonon heat conduction in superlattices," Phys. Rev. B **67**(19), 195311 (2003).
[53]A. Molina-Sanchez and L. Wirtz, "Phonons in single-layer and few-layer MoS_2 and WS_2," Phys. Rev. B **84**(15), 155413 (2011).
[54]W. Li, X. Chen, and S. Yang, "Phonon transport across coherent and incoherent interfaces," JOM **71**(11), 3885–3891 (2019).
[55]Y. Kyoung Ryu, R. Frisenda, and A. Castellanos-Gomez, "Superlattices based on van der Waals 2D materials," Chem. Commun. **55**(77), 11498–11510 (2019).